Basic aspects of Deep Lithography with Particles for the fabrication of micro-optical and micro-mechanical structures

Bart Volckaerts[a*], Pedro Vynck[a], Michael Vervaeke[a], Luigi Cosentino[b], Paolo Finocchiaro[b], Patrick Reichart[c], Gerd Datzmann[c], Andreas Hauptner[c], Günther Dollinger[c], Alex Hermanne[a] and Hugo Thienpont[a]

[a]Vrije Universiteit Brussel, Dept. of Applied Physics and Photonics (TW-TONA), Pleinlaan 2, 1050 Brussels, Belgium;

[b]INFN, Laboratori Nazionali del Sud, Via S.Sofia 44, 95125 Catania, Italy;

[c]Techn. Universität München, Physik-Department E12, James-Franck-Strasse, 85748 Garching, Germany

ABSTRACT

The strength of today's deep lithographic micro-machining technologies is their ability to fabricate monolithic building-blocks including optical and mechanical functionalities that can be precisely integrated in more complex photonic systems. In this contribution we present the physical aspects of Deep Lithography with ion Particles (DLP). We investigate the impact of the ion mass, energy and fluence on the developed surface profile to find the optimized irradiation conditions for different types of high aspect ratio micro-optical structures. To this aim, we develop a software program that combines the atomic interaction effects with the macroscopic beam specifications. We illustrate the correctness of our simulations with experimental data that we obtained in a collaboration established between the accelerator facilities at TUM, LNS and VUB. Finally, we review our findings and discuss the strengths and weaknesses of DLP with respect to Deep Lithography with X-rays (LIGA).

Keywords: micro-optics, micro-mechanics, micro-machining, deep lithography, plastics, ion stopping, dose simulations and optical surface profiles

1. INTRODUCTION

Mastering precision micro-structures in high-grade plastics for optical and mechanical applications has been the driving force for several research teams to develop and consolidate reliable fabrication techniques. Deep lithographic techniques with ionizing radiation sources are nowadays valid candidates to realize the stringent requirements of micro-components that can be easily embedded in high efficiency optical systems. Their basic principle relies on the accurate local modification of a positive resist layer using a projection mask, followed by a selective etching of the exposed zones. Ionizing radiation sources which induce sufficiently high absorbed doses to locally degrade the resist layer are deep UV-light, synchrotron X-rays and swift ion particles. In this contribution we will discuss the basic aspects behind Deep Lithography with Particles (DLP) as a candidate technology for the fabrication of high aspect ratio micro-structures. The idea behind DLP originated in the Department of Physics of the Friedrich-Alexander-Universität in the Erlangen-Nürnberg University where its proof-of-principle was demonstrated to realize plastic micro-optical basic components with collimated 8.5MeV proton beams[1–3] . Inspired by their results the institute for solid state physics at the Friedrich-Schiller-Universität in Jena performed several years later similar experiments while micro-machining mechanical test structures[4,5] . As an alternative to DLP with collimated proton beams, the nuclear physics group at the Oxford university explored the possibilities of 3MeV focused proton beams to micro-machine 10μm thin PMMA layers[6] . The promising outcome of this research resulted in spin-off activities at the physics department of the national university of Singapore where 2MeV focused proton beams are used for the fabrication of purely micro-mechanical components made in PMMA or SU8 material[7–10] . Since 1996, at the department of Applied Physics and Photonics of VUB, we have been upgrading this DLP technique for the fabrication of micro-optical structures dedicated to free-space parallel

* Corresponding author. E-mail: bvolckaerts@tona.vub.ac.be, Tel.: ++32 2 629 34 51, Fax: ++32 2 629 34 50

optical data-links and fiber-based interconnects[11, 12] . At present we are continuously improving its performances and extending its range of practical applications.

In general the DLP process consists of the following basic procedures : an ion irradiation of a PMMA-layer in well-defined regions, followed by either a development of the irradiated regions with a selective solvent or by a volume expansion of the bombarded zones caused by a diffusion of an organic monomer vapor. If needed, both processes can be applied to different regions of the same sample. Figure 1 illustrates the DLP process for a point-irradiated PMMA-sample where the proton beam is physically stopped by means of a fast mechanical shutter during each sample translation. As an alternative, the sample can be continuously moved in the beam according to a line pattern (not shown on figure 1).

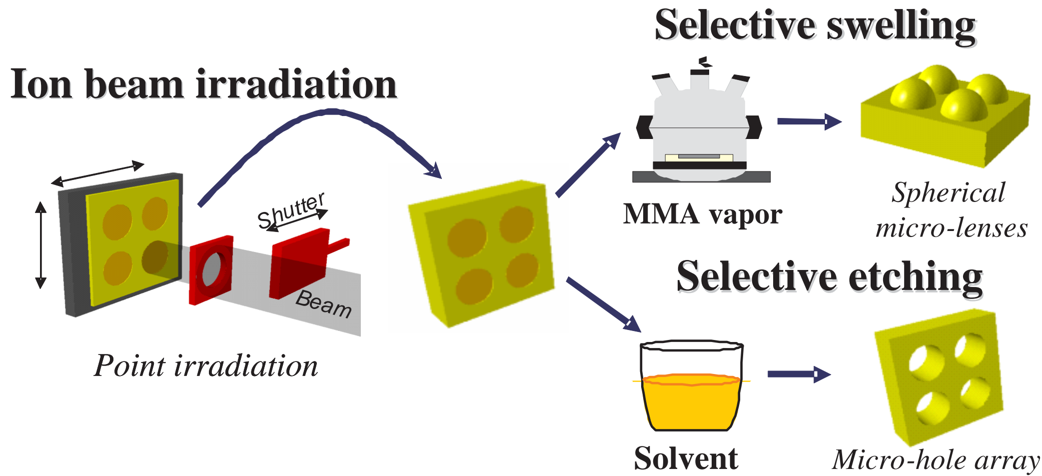

Figure 1. Schematic overview of the irradiation, development and lens-swelling process steps in the DLP-technology.

The concept of the process is based on the fact that proton irradiation of a sample, made of linear high molecular weight PMMA, will result in the rupture of the long polymer chains. As a consequence, the molecular weight of the material located in the irradiated zones will be reduced and free radicals will be created, resulting in material properties that are different from those of the bulk. The irradiated zones feature for instance a higher solubility than the bulk material. As a consequence they can be selectively etched using a special solvent (right bottom part of figure 1). This procedure allows for the fabrication of 2D arrays of micro-holes, rows of smoothly curved cylindrical micro-lenses and optically flat micro-mirrors and micro-prisms. Also alignment features and mechanical support structures can be fabricated with this procedure.

On the other hand, we can swell the irradiated domains using a monomer vapor (right upper part figure 1). Because of the much lower molecular weight of the PMMA material in the irradiated zones of the sample, the diffusion velocity for small molecules will be much larger there than in the non-irradiated material. This selective diffusion process will cause a considerable volume expansion of the irradiated area, which for circular footprints will result in hemi-spherical surfaces. After diffusion into the PMMA-sample the monomers will bond to the irradiation-induced free radicals and as a consequence will be fixed in the sample. This process permits the fabrication of stable spherical micro-lenses with well-defined heights[13] .

Recently we started up a collaboration at VUB with LNS and TUM started up a collaboration to investigate the possibilities of heavier ion particles and strongly-focused proton beams respectively to extend and improve the functionality of our present-day micro-structures[14–16] . We present in this contribution our first joint results while focusing on the fundamental interaction phenomena between different types of swift ions and resist molecules. We introduce in a first section the basic aspects of ion stopping in amorphous materials. This allows

us to predict the absorbed dose profiles in PMMA-substrates and the surface shape of the DLP components after chemical development. We perform here two case studies where respectively collimated and focused ion beams are used to expose thick PMMA-plates under different irradiation conditions. We will compare our findings that result from experiments that we obtained at the accelerator facilities of VUB, TUM and LNS. To conclude, we will will review and highlight the basic physical differences between deep lithography based on particle beams and the LIGA-technology based on X-rays[17–19] and give a survey of the advantages and drawbacks of DLP and LIGA for the fabrication of a wide range of micro-optical and micro-mechanical structures.

2. ION STOPPING IN PERSPECTIVES

The penetration of ionizing radiation like deep-UV light, X-rays and energetic ion beams modifies the material properties of targeted plastic slabs by a transfer of their energy to the molecular structure. While X-rays are entirely absorbed at once, ions will gradually lose their energy until they eventually stop inside the polymeric material. The electronic energy loss of ion particles are driven by Coulomb interactions and is frequently referred to as the electronic stopping power $\frac{dE}{\rho dx}$[20] . This parameter is defined as the energy loss dE of the interacting ion to the target per unit penetration depth dx and per mass density ρ.

In figure 2 we illustrate the energy transfer of several types of ion particles at different incident energies. We notice that the higher the particle energy, the deeper they will penetrate in the PMMA-target. We observe furthermore on the left hand side that 15MeV protons in Aluminium will stop after a much shorter distance than in PMMA. In the plot on the righthand side of figure 2, we show the impact of the ion mass on the 1D energy absorption curves in PMMA. For all ions we fixed the incident energy to 5MeV/u. From these graphs, we may conclude that the stopping power for heavier ions is higher in magnitude compared to light ion particles, which results in much shorter penetration depths of heavy ions. We mention here that alpha particles, or totally stripped Helium ions, stop at a comparable depth as proton particles with the same energy per nucleon.

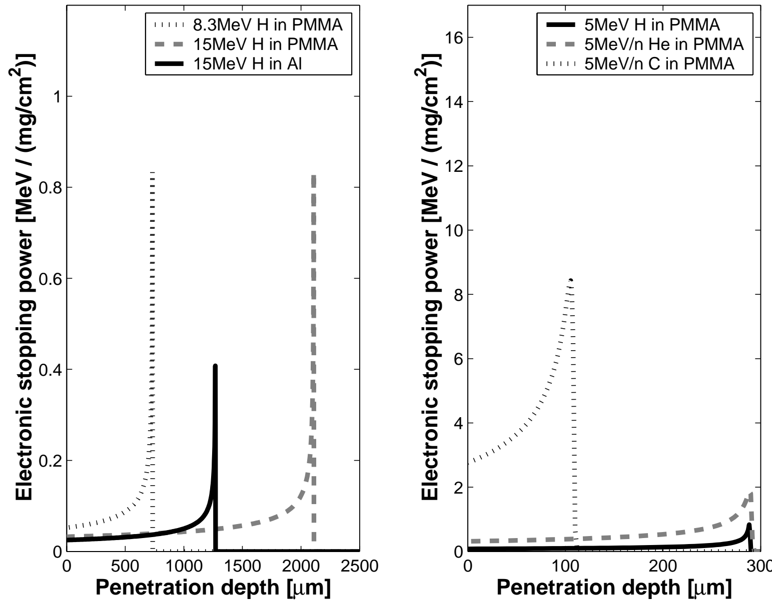

Figure 2. The stopping power of different ion particles in Aluminum and PMMA as a function of their penetration depth. The electronic stopping powers are taken from[21] .

This data will play a key-role in the prediction of the absorbed dose profiles in PMMA-samples.

Using the initial ion energy as a process parameter for tuning the stopping depth of the particles in the PMMA-plates, offers some perspectives for the fabrication of micro-structures. In particular, we consider the fabrication

of U-shaped positioning grooves with a depth of 125 μm for practical fiber alignment or micro-holes with a certain depth to precisely stop and fix a fiber in front of a monolithic integrated micro-lens as illustrated in figure 3.

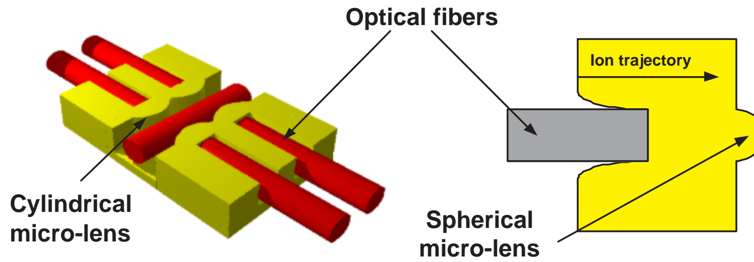

Figure 3. Principle drawing of fiber connector components fabricated with DLP that make use of the abrupt ion stopping effect. Left: 1D fiber connector with integrated cylindrical micro-lenses; Right: Monolithic fiber coupling element featuring a circular micro-hole and spherical micro-lens.

To illustrate the effect of abrupt ion stopping, we point irradiated a PMMA target with a 62MeV Carbon beam with a diameter of 500 μm. This experiment has been performed at the tandem accelerator of LNS, Catania. We applied Carbon fluences of 3.2 $10^5/\mu m^2$ which are high enough to completely develop the irradiated zones after 30min at 38° in GG-developer[22] . Because the depth of the created micro-holes corresponds to the ion range, we may conclude from figure 4 that 62MeV Carbon ions stop at 129 μm. Due to the abrupt stopping of the particles we were able during this experiment to obtain flat surfaces at the bottom of the micro-holes with a standard deviation smaller than 350nm. We executed a comparable experiment with a focused 70MeV Oxygen ion beam at the tandem accelerator of TUM, Munich. During this test we scanned with the beams an area of 200μm by 100μm and realized after 15 minutes under optimized etching conditions micro-holes with a mean depth of 83.5μm featuring a rms deviation of about 1μm. We described the etching process in[12] .

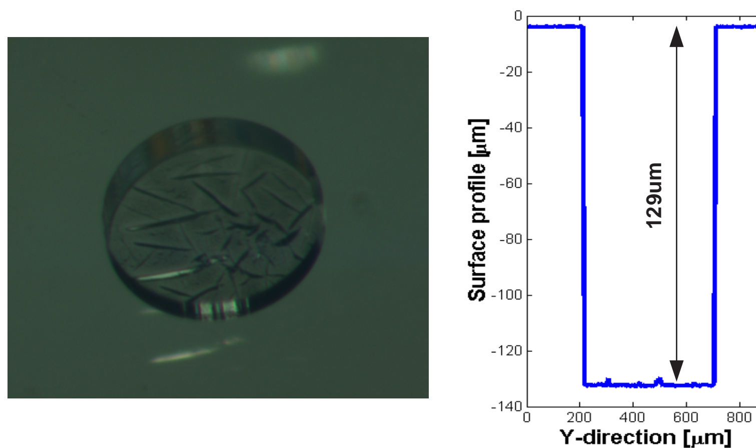

Figure 4. Picture and surface profile of a developed point-irradiated PMMA plate. The irradiation is performed with a 62MeV Carbon beam with a diameter of 500μm. We characterized the micro-hole with an optical non-contact profiler of the trademark VEECO.

3. DOSE CALCULATIONS IN ION EXPOSED PMMA-SAMPLES

Energy loss followed by degradation in locally irradiated PMMA-layers, is the physico-chemical cornerstone for the development of high-quality micro-opto-mechanical structures with DLP. The precise prediction of the 3D dose distribution in PMMA-samples under different irradiation conditions is therefore crucial to understand and

to optimize our technology. In this section we discuss the irradiation parameters that determine the absorbed doses in the target material.

The absorbed dose D is defined as the energy in kilo joule (kJ) absorbed per unit mass (g)[23] . It depends on the number of particles impinging on the sample and on the linear energy transfer of the ions in the target. The total number of ion particles per beam surface area S_{beam} perpendicularly oriented to the penetration trajectory of the ions is called *fluence (F)* and is given in units of $\#/\mu m^2$. In the DLP-technology typical ion fluences vary between $10^4/\mu m^2$ and $10^6/\mu m^2$ for Carbon ions and between $10^5/\mu m^2$ and $2\ 10^7/\mu m^2$ for protons. In practice, we determine this macroscopic beam parameter by integrating the ion beam current or intensity I_{beam} impinging on the PMMA-sample over the irradiation time t_{irr} :

$$F = \int_0^{t_{irr}} \frac{I_{beam} dt}{S_{beam} Q_1} \tag{1}$$

Here Q_1 denotes the charge state (in C) of the impinging ion. Depending on the experimental setup and the target geometry, we can measure the particle current on a metallic stopping probe located directly behind the PMMA sample. In case the particles are stopped in the target, we have to derive the fluence from the beam current measured on the last collimator in our irradiation setup. The second factor that influences the absorbed dose is the *linear energy transfer (LET)* of the particles which can be approximated for our purposes by the electronic stopping power $\frac{dE}{dx}$. The definition of the absorbed dose D in matter is then given by

$$D = F.\frac{dE}{dx} \tag{2}$$

4. DLP WITH COLLIMATED ION BEAMS : PREDICTING THE DEVELOPED SURFACE PROFILES

One of the most important characteristics that makes a mastering technique flexible, is its ability to precisely tune the surface profiles of the developed micro-structures. In the specific case of fiber connector components, for example, we are interested in the fabrication of *conical-shaped* mechanical alignment holes that facilitate the fiber insertion at the backside of the connector plate. On the other hand, *steep* surfaces with an optical quality are required in high-performance miniaturized prisms and cylindrical micro-lenses. In this section, we will investigate the physical limits of DLP when purely collimated ion beams are applied. To this aim we developed a software program that includes the single particles interaction behavior, like scattering and electronic energy transfer, in combination with the collective beam properties which are for collimated beams the beam divergence, the initial beam diameter and ion fluence. In our model we distinguish two interaction zones in the exposed material ; namely the PMMA-material interacting with the center part of the ion beam and, secondly, the edges of the exposed volume where the beam diameter deviations are important. In the central interaction part we assume dose depositions due to collimated ion beams with a uniform distribution. This is in a first approximation in agreement with practical DLP irradiation conditions where we only select the center part of the initial Gaussian ion beam. At the rim of the exposed zones, the beam divergence and multiple ion scattering influence the diameter deviation of the interacting ion beams, given by the relation

$$\Delta_{Total} = \sqrt{\Delta_{Scatt}^2 + \Delta_{Div}^2} \tag{3}$$

We derive here the beam diameter deviations after multiple scattering events Δ_{Scatt} according to the theory surveyed by[24] . In practical situations the beam divergence is determined by the magnetic lenses situating along the beam line for the realization of an efficient beam transfer. Because the accelerator settings differ slightly between two irradiation sessions, the magnets have to compensate this effect and hence the beam divergence changes accordingly. To verify the correctness of our program, we performed different irradiation sessions with proton beams at the cyclotron of VUB and with Carbon beams generated at the cyclotron of LNS, Catania.

In figure 5 we simulated the absorbed doses in PMMA-material after a (stationary) point exposure with a

collimated $120\mu m$ proton beam of 8.3MeV and a divergence of 17.5mrad. We assumed a relatively high proton fluence of 1.9 $10^7/\mu m^2$ to obtain a better illustration of the dose deviation inside the plate. We clearly observe that the swift protons gradually deposit higher doses the further they penetrate in the PMMA-plate, with a dose peak near the proton's stopping depth at $730\mu m$. This effect is due to the more intensive electronic interactions of the particles at the end of their trajectory, as we discussed in section 2. To derive the internal profile of the micro-holes after development, we calculate the location of the 0.9kJ/g dose line in the material (white line in figure 5). This value corresponds to the threshold dose at which the exposed PMMA-molecules can be removed after 1h at 38° in an ultra-sonic stirred GG-developer. This is in agreement with the critical doses for proton and X-ray exposures previously reported by[2] and[25, 26] , respectively. We found the critical etching dose to be 2kJ/g, in case no stirring is applied during the development. The righthand part of figure 5 illustrates the diameter variations of the micro-holes as a function of the ion's penetration depth. We observe a quasi linear increase in the first $500\mu m$ of the PMMA-plate, while a maximum diameter variation of $140\mu m$ is calculated near the proton stopping depth.

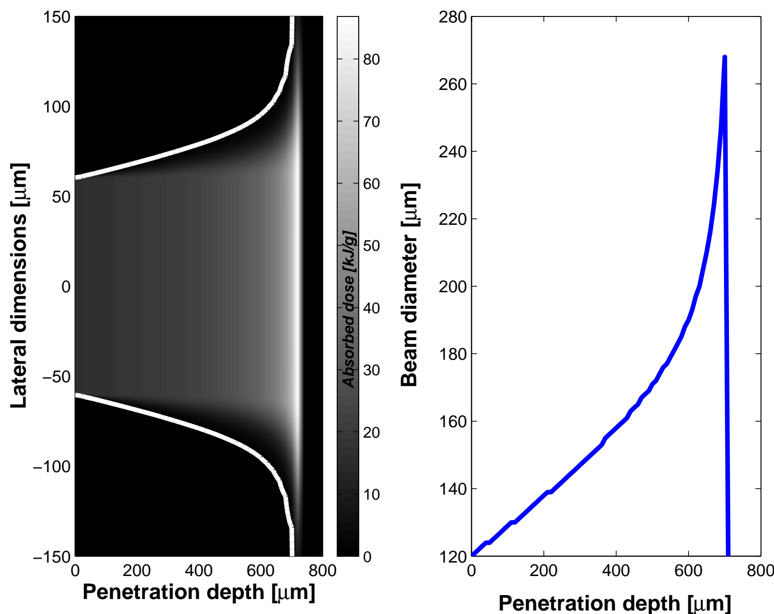

Figure 5. Cross section of the absorbed dose profile in a $800\mu m$ thick PMMA plate after a 8.3MeV proton irradiation (left plot). The initial proton beam has a diameter of $120\mu m$ and a divergence of 17.5mrad. We assumed a relatively high proton fluence of 1.9 $10^7/\mu m^2$. The surface profile after a selective development corresponds to the 0.9kJ/g dose line and is marked in white. The simulated diameter variations are given in the right graph.

We explore in figure 6 the propagation behavior of 62MeV/u Carbon beams and 8.3MeV, 16MeV and 34MeV proton beams through thick PMMA-plates. The proton and Carbon beams are generated at the cyclotrons of VUB and LNS, respectively, and the specific beam parameters are mentioned in table 1.

We observe the smallest diameter deviations of $50\mu m$ over a length of 5mm when 62MeV/u Carbon beams are applied. This is due to the small multiple scattering angles of swift heavy ions in matter. Under the assumed irradiation conditions we observe three times larger diameter deviations for 34MeV proton beams, however this ratio changes when different ion fluences are deposited in the PMMA-plate. This means that swift Carbon beams are excellent candidates for the fabrication of deep, flat surfaces integrated in miniaturized prisms or cylindrical micro-lenses. Proton beams, on the other hand, give rise to larger diameter deviations. They exhibit the possibility to fabricate dense fiber alignment structures featuring micro-holes with conical-shaped internal sidewalls. We observe that the experimental diameter deviation at the particle's stopping depth is smaller than derived in our calculations. This is due to the fact that our software code does not include range straggling effects caused by the finite energy distribution of the original accelerated proton beams and the stochastic character of the

Ion particles	Fluence $[\#/\mu m^2]$	Simulation parameters			Experimental conditions
		θ_{div} $[mrad]$	ϕ_{coll} $[\mu m]$	D_{crit} $[kJ/g]$	Stirrer used?
8.3MeV H+	10^6 to 2 10^7	17.5	120	0.9	Yes
16MeV H+	1.05 10^7	6.06	170	0.9	Yes
34MeV H+	1.3 10^7	9.3	860	2	No
62MeV/u C+	2.69 10^6	5.79	863	2	No

Table 1. Overview of investigated ion beams, the considered simulation parameters (beam divergence θ_{div}, collimated beam diameter ϕ_{coll} and critical etching dose D_{crit}) and the experimental stirring conditions.

energy transfer.

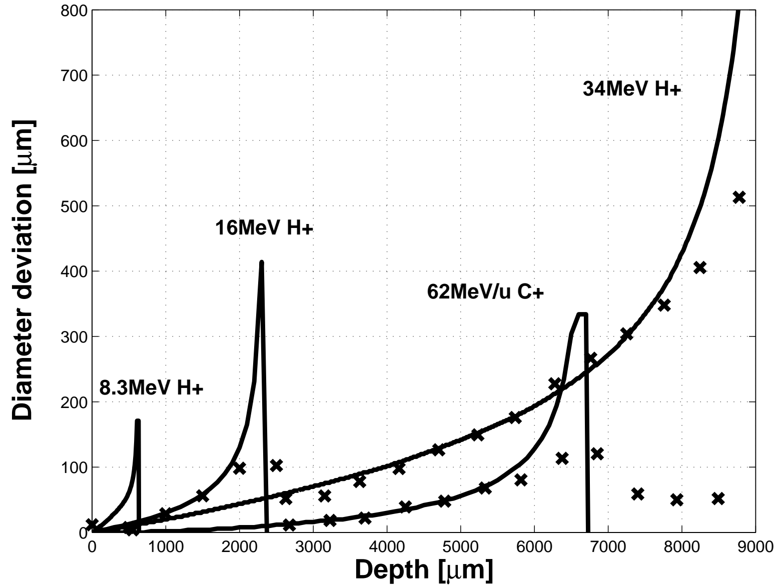

Figure 6. The diameter deviations of developed micro-holes after different ion beam exposures : A comparison between experimental (crosses) and simulated (solid lines) data. Specific information of the considered interactions are summarized in table 1.

The impact of the proton fluence on the conical surface profile of micro-holes is shown in figure 7. We consider here 8.3MeV proton beams with a diameter of $120\mu m$ travelling through a $500\mu m$ thick PMMA-plate. If larger proton fluences are deposited on the PMMA material, the scattering effect will be enhanced in the shadow zones of the dose profiles. This results in larger diameters at the exit surface of the PMMA-plate, after $500\mu m$ of penetration. This means that if we need to fabricate high aspect-ratio components with flat surfaces, we have to deposit small proton fluences. Conical fiber insertion features, on the other hand, ask for high proton fluences to enhance the multiple scattering effect in the bombarded plate. Because the diameter deviations saturate for high proton fluences, we can neglect the benefit of proton fluences higher than 2 $10^7/\mu m^2$. We currently use the proton fluence as a key process parameter to optimize the surface profiles of fiber connector components in[27] .

We observe in this section a good agreement between the calculated diameter deviations and experimental data we achieved at the cyclotron facilities of VUB and LNS. We can therefore conclude that our software program

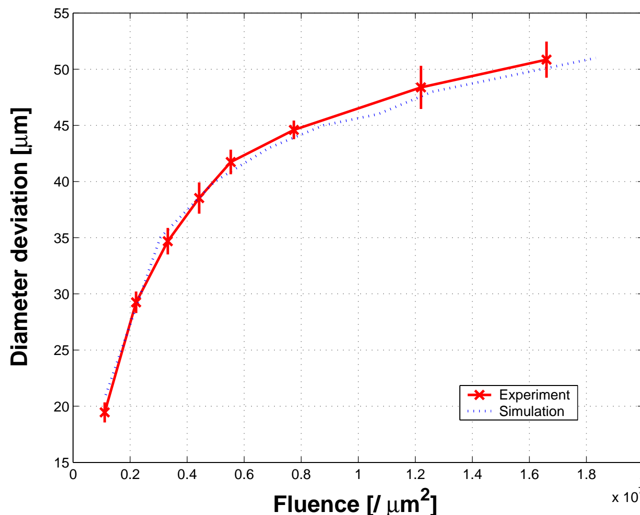

Figure 7. Diameter deviations at the backside of a $500\mu m$ thick PMMA-plate that is exposed with a $120\mu m$ circular proton beam. A good agreement between the simulations and the experimental results has been obtained.

provides a powerful and fast tool to simulate the impact of the most important DLP irradiation parameters on the surface flatness of the fabricated micro-structures.

5. DLP WITH STRONGLY-FOCUSED ION BEAMS

From our previous discussions we know that a shift from 8.3MeV proton beams[28] towards higher energies offers several advantages for the fabrication of high aspect ratio micro-structures in thick resist layers. A drawback however is the requirement for thicker masks, that completely stop the particles, featuring aperture sizes corresponding to the smallest sizes present of the targeted micro-structure. In case of fiber connector components these critical dimensions equal the diameter of the circular alignment holes of $125\mu m$. If smaller clamping mechanisms are included in the design, smaller beam diameters hence smaller stopping apertures are required. Since the range of 17MeV protons in Aluminium is about 2mm, this means that masks with aspect ratios of 20 or higher with ultra-flat internal sidewalls are necessary for these DLP purposes. The realization of such specifications is not straightforward for today's micro-machining techniques and still asks for further improvements. From this viewpoint we started a collaboration with the physics department E12 at TUM to study the perspectives of DLP with 17MeV focused proton beams, where no beam collimation is needed near the PMMA target[16] . Furthermore, a focused beam line offers the advantage that relative low beam current (below 1nA) are bundled in small spots with high proton densities. This reduces the activation of the irradiation setup and limits the noise signal during the in-situ fluence measurement to a strict minimum. A description of the beam line and focusing setup at TUM is given in[29, 30] .

During our experiments we explored two irradiation modes. In a first approach, we scanned a focused beam with characteristic diameters of about $5\mu m$ according to a rectangular plane with feature sizes of $125\mu m$. Here, the accuracy of the micro-structures is related to the precision of the magnetic scanning system. The left picture in figure 8 shows a developed rectangular micro-hole in a 2mm thick PMMA-plate with characteristic sizes of $125\mu m$. In a second approach we irradiated point arrays with different proton fluences and different focus parameters (right picture). After each point, an ultra fast electrostatic shutter stopped the beam and a sample manipulator translated the PMMA-sample to the next position. The accuracy of this second irradiation mode is determined by the precision of the translation stage.

To investigate the internal surface profiles of the developed micro-holes, we irradiated a target that consisted of several stacked $500\mu m$ thick PMMA plates with a 17MeV focused proton beam of 240pA. We characterized the

Figure 8. Rectangular and circular micro-holes developed in collaboration with TUM by means of a focused 17MeV proton beam. The pictures are taken under a tilted angle allowing to observe the internal conical surface profiles of the respective micro-structures.

diameter increase of the micro-holes after each $500\mu m$ with a calibrated microscope and found three interesting irradiation regimes depending on the sample position with respect to the focus point of the proton beam. Figure 9 shows these three working regimes and illustrates the advantages of strongly focused proton beams to extend the variety of our today's DLP-structures.

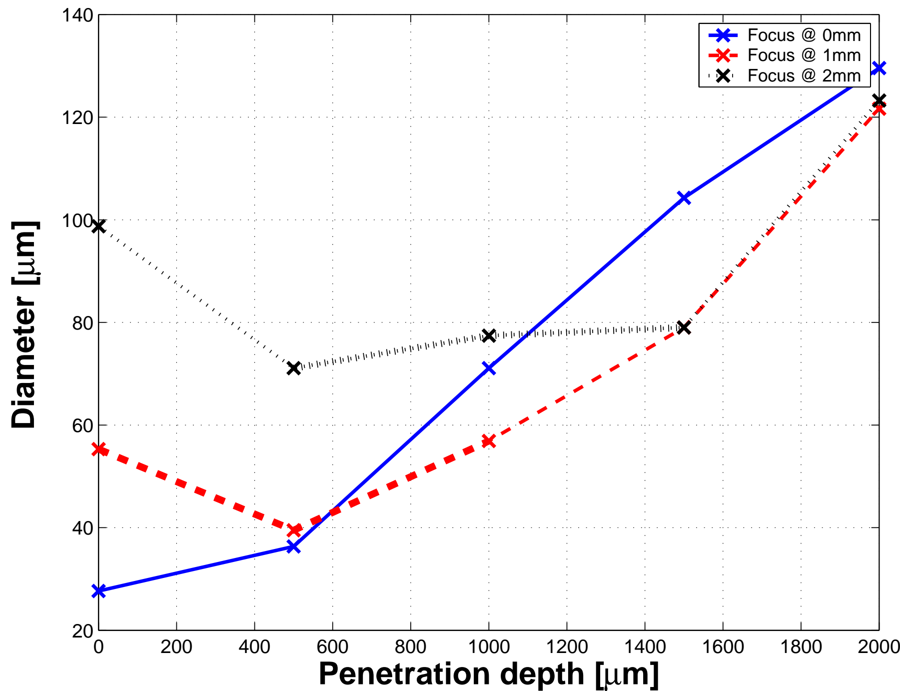

Figure 9. Micro-hole fabrication with focused proton beams at TUM : The impact of the sample position on the developed internal surface profiles (Focus @ 0mm : The entrance surface of the sample corresponds to the focus point of the proton beam, focus @ 1mm : Focus point is situated at 1mm inside the PMMA sample, ...). The interesting working regimes are marked in bold lines.

In a first regime, the entrance surface of the PMMA-target corresponds to the focus point of the beam. We hereby use the large beam divergences of the focused beams to enhance the diameter variations of the micro-holes. In this irradiation mode the focused proton beams are excellent candidates to fabricate fiber alignment holes with highly conical profiles to establish an easier fiber insertion. Furthermore, these proton beams allow to integrate ultra-small springs or notches at the rim of fiber alignment holes to establish an additional mechanical fixation.

A second irradiation regime, where the focus point of the beam is situated 1mm inside the target, is shown by the dashed line in figure 9. Under these conditions a curved surface is created along the first millimeter of the target. We can take advantage of this effect during the fabrication of a monolithic fiber butt connector where light has to be coupled between two fibers under an angle of 180° (figure 10). In this component the divergence of the light beam originating from the entrance fiber is compensated in one direction by a cylindrical micro-lens and in the perpendicular direction by means of a reflective curved surface. The cylindrical micro-lenses can be fabricated by translating the PMMA-plates during the irradiation according to a curved pattern[31] , while the curved reflective surface will be created after tuning the focus punt of the proton beam in the target. The reflective surface walls will be realized after a local deposition of a reflection coating.

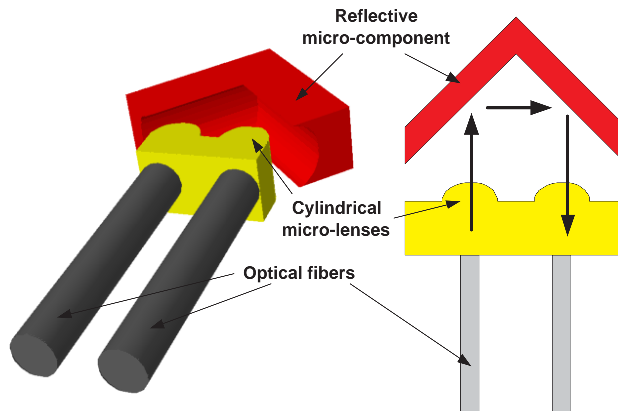

Figure 10. Principle drawing of a fiber butt connector created by means of focused swift proton beams.

A last irradiation regime in which focused proton beams can offer advantages compared to collimated beams is observed when the focus point is situated 2mm inside the PMMA-target. In this case, the beam shape locally compensates the effect of multiple proton scattering such that optical surface walls with improved flatness are created at target depths between $500\mu m$ and $1500\mu m$.

To further explore the advantages of focused ion beams, we will install by the end of the year 2004 a quadrupole triplet with a field strength of each lens of 20T/m at the end of one of the VUB cyclotron beam lines. This will allow us to investigate the reliability and the optical performances of a new generation micro-structures at the accelerator sites of TUM and VUB using focused proton beams with energies between 5MeV and 40MeV.

6. CONCLUSIONS : A COMPARISON BETWEEN DLP AND LIGA

Although it might seem an easy task to structure transparent bulk materials in such a way as to obtain a dedicated optical functionality, the number of accurate mastering techniques for the fabrication of micro-optical and micro-mechanical systems is rather scarce. In this contribution we studied the impact of the irradiation parameters on the surface quality of micro-structures which are fabricated with DLP. To this aim we developed in section 4 a software program that includes the effect of single ion interactions, combined with the macroscopic beam specifications like the divergence, the ion fluence and the beam diameter. We observed a good agreement between our simulation results and the experimental data we obtained at the cyclotron site of VUB, at the tandem and cyclotron site of LNS and at the focused beam line of TUM. We may therefore conclude that the software program is an excellent candidate to predict the different characteristics of the developed micro-structures while avoiding time-consuming and expensive irradiation sessions. The program additionally allows us to perform a strength and weakness analysis of our DLP technology and provides the user the required information to decide whether DLP offers special benefits with respect to other micro-machining technologies. As a case study, we will now compare the advantages of DLP with those of LIGA for the fabrication of micro-optical and micro-mechanical structures.

A first characteristic parameter is the *thickness* of the micro-structure which is, for deep lithographic technologies like DLP and LIGA, directly related to the maximum penetration depth of the ionizing radiation. Large storage rings for electron beams with energies above 5GeV, like for example the European Synchrotron Radiation Source in Grenoble, deliver high energetic X-rays with corresponding ranges above 1cm[26] . These magnitudes are comparable to the typical ranges of 34MeV proton beams which can be accelerated at the VUB cyclotron facility. Apart from a purely scientific point of view, the advantages to fabricate "micro" structures with much higher thicknesses are limited and can't be in general defended because of its high cost. Indeed, once optical structures have macroscopic geometries, there exist alternative, low-cost techniques which are valuable to fabricate components in plastic, glass or metals.

A second important parameter is the *surface flatness* of the developed micro-components. It is evident that the slightest tilt of the optical sidewalls directly results in a deviation of the propagation direction of the light beam through the optical system, accompanied with crosstalk and an important drop in coupling efficiency. The only physical effect that drastically influences the surface flatness of DLP-components is multiple ion scattering. Limited by this effect, we can expect maximum aspect ratios of our DLP-structures of 100:1. Due to their much smaller scattering cross sections, the straggling of X-rays is orders of magnitudes smaller than for ion particles. This results in the fabrication of ultra-flat side facets with deviations smaller than 1μm over depths of several millimeters[32, 33] . We therefore conclude that Deep X-ray Lithography is the ultimate technology to create optical pathway blocks with a high optical throughput that consists of micro-mirrors and cylindrical micro-lenses. On the other hand, in case one aims at fabricating fiber connector components with conical profiles, we can directly take advantage of the ion scattering effects. Depending on the functionality of the developed micro-system, we can enhance or reduce this effect by fine-tuning the absorbed dose profiles and etching parameters. To achieve this type of conical profiles with X-ray lithography, one has to tip and tilt the resist layer in the beam.

Furthermore, the physical properties of charged particles offer some particular advantages with respect to X-rays. We can indeed modify the shape of the ion beam with the aid of strong magnetic lens systems. As we have proven in collaboration with the E12 department of the TUM in Munich, these kind of magnets allow to narrow the spot size of ion beams down to several micrometers and is an attractive alternative to directly write a design into the resist without making use of a thick collimator or projection mask. The settings of the magnetic lens system define in this approach the size of the ion beam. As we discussed in section 2, another interesting property of ions is their abrupt stopping behavior in the matter, offering the possibility to construct real 3D micro-structures by tuning the particle's energy during the same irradiation session. We will extend this study in the near future to explore the possibilities of DLP with collimated and focused ion beams for the fabrication of more complicated 3D opto-mechanical micro-systems with innovative applications in photonics.

ACKNOWLEDGMENTS

This research is made possible through the financial support of the Fund for Scientific Research-Flanders (FWO-Vlaanderen), the IAP Photon Network, the Institute for the Promotion of Innovation by Science and Technology in Flanders (IWT), the IWT ITA-II and GBOU project "VLSI Photonics" and the Research Council (OZR and GOA) of the VUB. Bart Volckaerts is indebted to IWT for his research fellowship and for financial support. The authors thank the INFN Gruppo V for its financial support to the SIMPLE experiments.

REFERENCES

1. K.H. Brenner et al, Applied Optics, Vol.29, Nr.26, pp.3723-3724 (1990)
2. S. Kufner, *3D-Integration miniaturisierter refraktiver optischer Komponenten in PMMA*, PhD dissertation at the Friedrich-Alexander-Universität Erlangen-Nürnberg (1993)
3. M. Kufner, *Herstellung und Charakterisierung von hochgeöffneten Mikrolinsen in PMMA*, PhD dissertation at the Friedrich-Alexander-Universität Erlangen-Nürnberg (1993)
4. F. Schrempel et al, NIMB, Vol.132, pp.430-438 (1997)
5. F. Schrempel et al, NIMB, Vol.139, pp.363-371 (1998)

6. M.B.H. Breese et al, NIMB, Vol.77, pp.169-174 (1993)
7. S.V. Springham et al, NIMB, Vol.130, pp.155-159 (1997)
8. J.L. Sanchez et al, NIMB, Vol.136-138, pp.385-389 (1998)
9. J.A. van Kan et al, NIMB, Vol.148, pp.1085-1089 (1999)
10. T. Osipowicz et al, NIMB, Vol.161-163, pp.83-89 (2000)
11. H. Thienpont et al, Proc. of the IEEE, Vol.88, No6, pp.769-779 (2000)
12. B. Volckaerts et al, Asian Journal of Physics, Vol. 10, No. 2, pp. 195-214 (2001)
13. H. Ottevaere et al, J. opt. A: Pure Applied Optics, Vol.4, pp.S22-S28 (2002)
14. Proposal for beam time at LNS, presented by B. Volckaerts et al in November 2002. We executed the experiments in May and July 2003.
15. Proposal for beam time at LNS, presented by B. Volckaerts et al in November 2003. The experiments are planned in the first period of 2004.
16. Proposal for beam time at TUM, presented by B. Volckaerts et al in January 2002. We executed the experiments in June 2002.
17. E.W. Becker et al, Naturwissenschaften, Vol.69, pp.520-523 (1982)
18. R. Ruprecht et al, Microsystem technology, Vol.4, pp.28-31 (1997)
19. H. Guckel, Proc. of the IEEE, Vol.86, No.8, pp.1586-1593 (1998)
20. M. Nastasi, J.W. Mayer and J.K. Hirvonen, *Ion-solid interactions, Fundamentals and applications*, Cambridge Solid State Science Series, Canbridge University Press (1996)
21. J.F. Ziegler and J.P. Biersack, *SRIM : The stopping and range of ions in matter*, Version SRIM-2003.05, Shareware available on SRIM.com (2003)
22. F.J. Pantenburg et al, NIMB, Vol.97, pp.551-556 (1995)
23. J.R. Greening, *Fundamentals of radiation dosimetry*, Medical physics handbook, Vol.15, second edition, Adam Hilger Ltd, Bristol and Boston (1981)
24. W.T. Scott, Rev. Mod. Phys., Vol.35, Nr.2, pp.231-313 (1963)
25. H. Zumaqué et al, J. Micromech. Microeng., Vol.7, pp.79-88 (1997)
26. G. Feiertag et al, J. Micromech. Microeng., Vol.7, pp.323-331 (1997)
27. B. Volckaerts et al, Contribution to the MEMS, MOEMS, and micromachining conference, part of Photonics Europe, SPIE, 26-30 April 2004, Strasbourg, France, Manuscript number 5455-34
28. P. Vynck et al, Proceedings Symposium of the IEEE/LEOS Benelux Chapter, Amsterdam, The Netherlands, pp.298-301 (2002)
29. G. Hinderer et al, Contribution to the 5th Int. Conf. on nuclear microprobe technology and applications, Nov. 10-16, Santa Fe, NM, USA (1996)
30. G. Datzmann et al, NIMB, Vol.181, pp.20-26 (2001)
31. B. Volckaerts et al, Proceedings Symposium of the IEEE/LEOS Benelux Chapter, Brussels, Belgium, pp.69-72 (2001)
32. W. Ehrfeld et al, J. Vac. Sci. Technol. B, Vol.16, No.6, pp.3526-3534 (1998)
33. A. Ting, Sandia report, SAND2001-8366 (2001)